



## Pressure-induced electronic topological transitions in the charge-density-wave material In<sub>4</sub>Se<sub>3</sub>

Yuhang Zhang <sup>a,b</sup>, Liyan Song <sup>a</sup>, Xuecheng Shao <sup>a</sup>, Yan Li <sup>a</sup>, Pinwen Zhu <sup>a,\*</sup>, Huailiang Xu <sup>b,\*\*</sup>, Junyou Yang <sup>c,\*\*\*</sup>

<sup>a</sup> State Key Laboratory of Superhard Materials, College of Physics, Jilin University, Changchun 130012, China

<sup>b</sup> State Key Laboratory on Integrated Optoelectronics, College of Electronic Science and Engineering, Jilin University, Changchun 130012, China

<sup>c</sup> State Key Laboratory of Materials Processing and Die & Mould Technology, Huazhong University of Science and Technology, Wuhan 430074, China



### ARTICLE INFO

#### Article history:

Received 3 January 2017

Received in revised form

29 March 2017

Accepted 24 April 2017

Available online 1 May 2017

#### Keywords:

In<sub>4</sub>Se<sub>3</sub>

High-pressure

Electronic topological transition

Structural transition

Charge-density-wave

Thermoelectric property

### ABSTRACT

High-pressure *in situ* angle dispersive X-ray diffraction (ADXRD) measurements were performed on the charge-density-wave (CDW) material In<sub>4</sub>Se<sub>3</sub> up to 48.8 GPa. Pressure-induced structural changes were observed at 7.0 and 34.2 GPa, respectively. Using the CALYPSO methodology, the first high-pressure phase was solved as an exotic *Pca*<sub>2</sub><sub>1</sub> structure. The compressional behaviors of the initial *Pnnm* and the *Pca*<sub>2</sub><sub>1</sub> phases were all determined. Combined with first-principle calculations, we find that, unexpectedly, the *Pnnm* phase probably experiences twice electronic topological transitions (ETTs), from the initial possible CDW state to a semimetallic state at about 2.3 GPa and then back to a possible CDW state at around 3.5 GPa, which was uncovered for the first time in CDW systems. In the both possible CDW states, pressure provokes a decrease of band-gap. The observation of a bulk metallic state was ascribed to structural transition to the *Pca*<sub>2</sub><sub>1</sub> phase. Besides, based on electronic band structure calculations, the thermoelectric property of the *Pnnm* phase under compression was discussed. Our results show that pressure play a dramatic role in tuning In<sub>4</sub>Se<sub>3</sub>'s structure and transport properties.

© 2017 Elsevier B.V. All rights reserved.

## 1. Introduction

For decades, more and more attention is being focused on the CDW materials induced by quasi-one-dimensional lattice distortion (Peierls distortion) [1–3]. Because the occurrences of CDW order is well established in essentially all underdoped cuprates high-temperature superconductors (HTSCs) [4–18]. In addition, since CDW materials have been used as model systems for the understanding of the interplay among electrons, phonons and spins in strongly coupled electron–lattice systems [19].

It is known that the orthorhombic lattice structure (space group *Pnnm*) of In<sub>4</sub>Se<sub>3</sub> is a CDW material under ambient conditions [20–22]. It contains quasi-two-dimensional layers stacked with weak interaction of van der Waals type along *a* direction, as seen in Fig. 1. Within the layer, (In1-In2-In3)<sup>5+</sup> multivalent clusters are

connected with Se atoms by ionic-covalent bond, forming In–Se–In zigzag chains along the *c* axis [21,23]. In<sub>4</sub>Se<sub>3</sub> has been thought to be suitable for fabrication of infrared optical fiber and nanowires [24–26], and applications of photovoltaic advices [27–29]. Furthermore, recently, excellent thermoelectric figure of merit *ZT* value of 1.48 at 705 K was achieved in single crystalline In<sub>4</sub>Se<sub>3-x</sub>, due to its extremely low thermal conductivity [20].

Pressure was recognized to be the cleanest method for tuning crystalline structures and the physical properties of these CDW compounds. For examples, pressure significantly raises the superconducting transition temperature *T<sub>c</sub>* in almost established CDW compounds [30–42]. However, the precise nature of the CDW and its relationship with superconductivity is unclear [1,43]. Moreover, in particular, pressure-induced ETT, a modification of the topology of the Fermi surface, can result in significant enhancements of thermoelectric properties in strongly correlated systems [44–52]. Besides, Schwarz et al. reported that In<sub>4</sub>Se<sub>3</sub> undergoes a structural transition at 8.8 GPa, while the structure of the high-pressure phase is still unknown [53]. Therefore, it is important to explore the structure and transport properties of In<sub>4</sub>Se<sub>3</sub> by applying pressure, in order to find a better candidate for thermoelectric devices and

\* Corresponding author.

\*\* Corresponding author.

\*\*\* Corresponding author.

E-mail addresses: zhupw@jlu.edu.cn (P. Zhu), huailiang\_xu@jlu.edu.cn (H. Xu), jyyang@mail.hust.edu.cn (J. Yang).

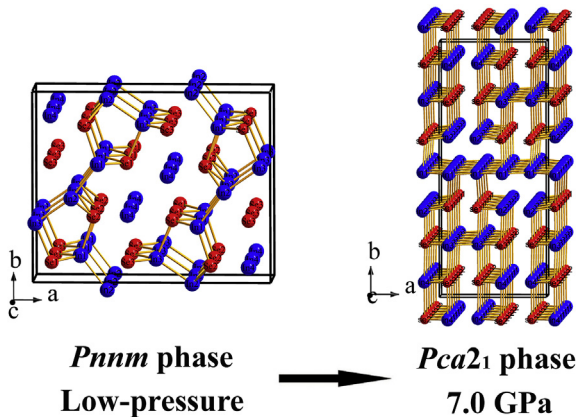


**Fig. 1.** Schematic representation of the *Pnnm* and *Pca<sub>2</sub>1* phases.

offer a platform for the exploration of novel superconductors.

Here, we report on the possible pressure-induced ETTs and structural transitions in  $\text{In}_4\text{Se}_3$ , for the first time, by *in-situ* high-pressure ADXRD measurements, using a diamond anvil cell (DAC), in conjunction with first-principles calculations.

## 2. Experimental details

In our experiments, purity  $\text{In}_4\text{Se}_3$  powder was provided by Yang et al. [54]. Pressure was generated by a symmetric DAC with 300  $\mu\text{m}$  diamond culet size. The powder was loaded in a 120  $\mu\text{m}$  diameter hole drilled in the T-301 stainless steel gasket and chips of ruby were added as pressure calibrator [55]. A methanol-ethanol-water (16:3:1) mixture was employed as the pressure transmitting medium. *In situ* high-pressure ADXRD experiments were performed at the beamline X17C of the National Synchrotron Light Source (NSLS) using a monochromatic wavelength of 0.4095  $\text{\AA}$ . The average acquisition time was 300 s. The integration to conventional  $2\theta$ -intensity data was carried out with the FIT2D software [56]. Rietveld refinements were performed using the GSAS-EXPGUI package [57,58].

We performed structure prediction through a global minimization of free energy surfaces merging ab initio total-energy calculations via CALYPSO methodology [59]. For the first-principles calculations, the density functional theory with the Perdew-Burke-Ernzerhof exchange-correlation as implemented in the Vienna Ab initio Simulation Package (VASP) code [60] and the generalized gradient approximation (GGA) [61] is implemented on a projector augmented wave (PAW) basis [62,63]. The PAW method based upon the frozen core approximation with  $5s^25p^1$  and  $4s^24p^4$  electrons as valence for In and Se, respectively, was adopted. Integration in the Brillouin zone was performed using special  $k$  points generated with  $4 \times 4 \times 4$  mesh parameter grids. Convergence tests give a kinetic energy cutoff as 300 eV, ensuring convergence of the total energy within  $10^{-3}$  meV/atom. The lattice parameters were directly taken from the Rietveld refinement. The theoretical atomic positions are electronically relaxed based on the experimental atomic positions.

## 3. Results and discussion

The selected ADXRD patterns are shown in Fig. 2 and S1. It can be seen that the first and second pressure-induced structural transitions of  $\text{In}_4\text{Se}_3$  started at about 7.0 and 34.2 GPa, respectively, where new peaks appeared. Decompression experiment shows that structural transition was irreversible, see Fig. 2. As can be seen in Fig. 3a and b, Rietveld refinements of ADXRD patterns clearly

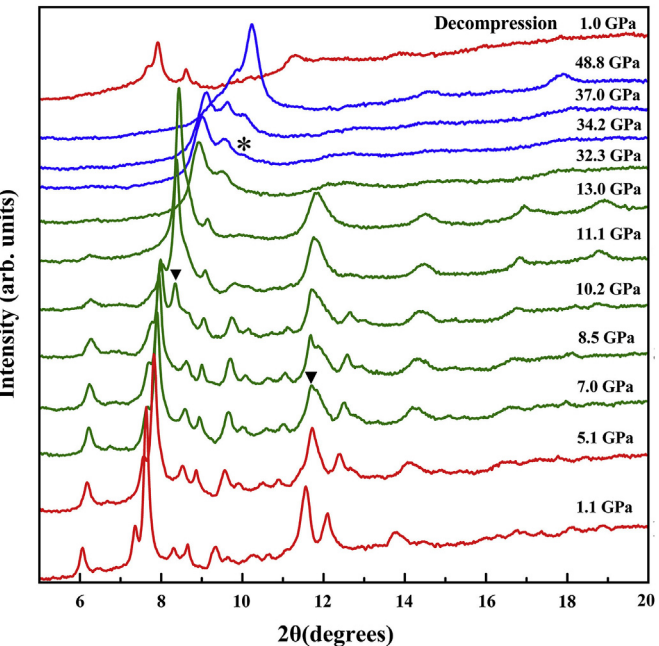


**Fig. 2.** Angle dispersive X-ray powder diffraction patterns of  $\text{In}_4\text{Se}_3$  under high pressure at room temperature. Arrow and asterisk represent new diffraction peaks.

illustrate that the initial *Pnnm* phase is still stable at 5.1 GPa. The detailed refinement results, such as lattice parameters and atomic coordinates, are shown in the *Supplementary Material*. Fig. 2 clearly illustrates that the first structural transition is not completed up to 13.0 GPa. To solve the crystal structure of the first high-pressure phase, the structure prediction via CALYPSO methodology was performed [59] and the best fitting was achieved for an exotic orthorhombic structure (space group *Pca<sub>2</sub>1*). Fig. 3c shows the Rietveld refinement for the *Pca<sub>2</sub>1* phase at 20.2 GPa, which has a good fitting with the ADXRD pattern. The relative experimental results of Rietveld refinement were located in the *Supplementary Material*.

During the compression process from 1.1 to 3.5 GPa, the ( $\text{In}_1\text{-}\text{In}_2\text{-}\text{In}_3$ ) clusters show nearly straight at 2.3 GPa, which leads to the quasi-two-dimensional layers all connected by the formation of  $\text{In}_2\text{-Se}_3$  bonds at that pressure (see Fig. S2). The detailed bond lengths in *Pnnm* structure are located in *Supplementary Material*. The schematic representation of the *Pca<sub>2</sub>1* phase of  $\text{In}_4\text{Se}_3$  is located in Fig. 1 and S3. It is indicated that the *Pca<sub>2</sub>1* structure is built up of stacking  $a\text{-}c$  plane layers of rhombus network of  $\text{In}_1$  atoms along  $b$  axis. Between two close  $\text{In}_1$  atoms layers, the warped  $b\text{-}c$  plane network layers consisting of  $\text{In}\text{-Se}$  ionic-covalent bonds are piled along  $a$  direction.

The evolution of the cell parameters in *Pnnm* phase is presented in Fig. 4. The contraction of the lattice parameters is anisotropic. It can be seen that  $a$  direction are more compressible than  $b$  and  $c$  directions, which is due to the weak intermolecular bond along  $a$  direction and strong covalent-ionic interactions within the warped  $b\text{-}c$  plane layers. For the overlapping diffraction peaks in the pressure region of mixed phases, it is difficult to identify the peak positions exactly. Therefore, we only display the lattice parameters of the *Pca<sub>2</sub>1* phase at above 13.0 GPa.

The volume per four formula units as a function of pressure is shown in Fig. S4. These  $P\text{-}V$  data are fitted to the usual Birch-Murnaghan (BM) equation of state (EOS) [64]. By fixing first-pressure derivative  $B_0' = 4$ , we obtained  $B_0$  of 47.2(8) GPa and  $V_0 = 775.16(4)$   $\text{\AA}^3$  for the *Pnnm* phase. The lower  $B_0$  is likely

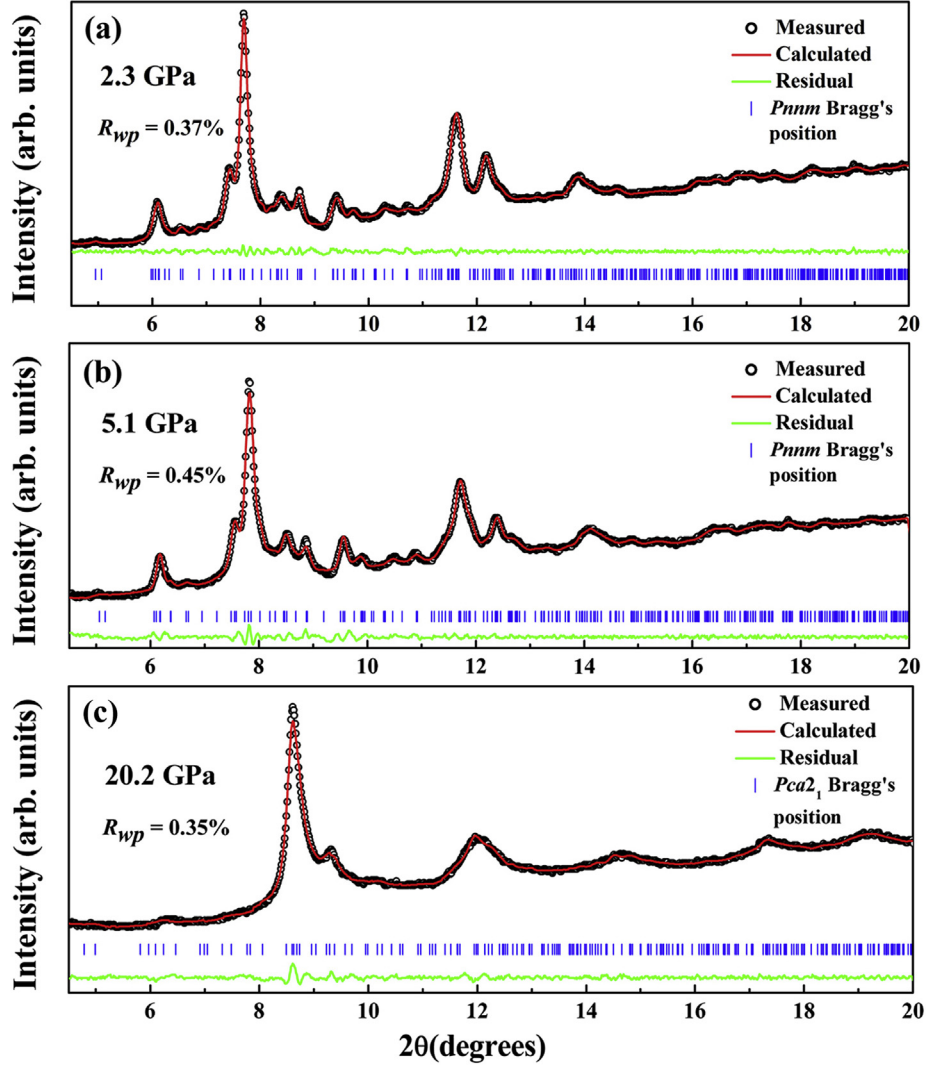


**Fig. 3.** Rietveld refinement results of (a) 2.3, (b) 5.1 and (c) 20.2 GPa, respectively.

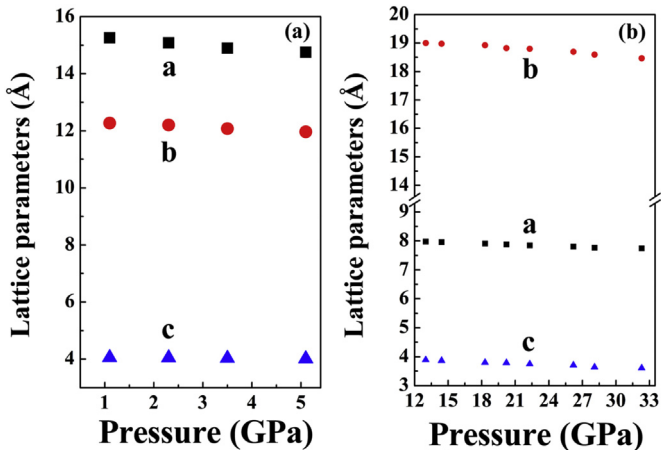


**Fig. 4.** (a) cell parameters of *Pnnm* phase, (b) lattice parameters of the *Pca2*<sub>1</sub> phase. Errors given by the GSAS EXPGUI package are smaller than the marker sizes.

originating from the high compressibility of *a* direction. The compression behavior of the *Pca2*<sub>1</sub> phase is determined by the following characteristic parameters:  $B_0 = 64.8(3)$  GPa,

$$V_0 = 685.72(4) \text{ Å}^3 \text{ and } B'_0 \text{ fixed to 4 (see Fig. S4).}$$

In order to determine the electronic band structures of  $\text{In}_4\text{Se}_3$  at different pressures, we carried out first-principles calculations. As shown in Fig. 5a, the *Pnnm* phase is a direct band-gap semiconductor ( $E_g = 0.30$  eV) at ambient pressure, with the conduction-band minimum (CBM) and valence-band maximum (VBM) located at  $\Gamma$  point. The significant hole band dispersion is observed along the  $\Gamma$ -Y symmetry line, indicating that the hole conduction path is mainly along the *a* direction. From Fig. 5b, the electronic structure of the *Pnnm* phase at 1.1 GPa is similar to that of ambient pressure, but the band-gap decreases to 0.17 eV. The partial electron density of state (PDOS) and sum DOS results of 1.1 GPa indicate that VBM is mostly dominated by the contributions of In4-s, Se3-p, Se2-p and Se1-p states, as shown in Fig. S5a. The ETT is a consequence of a topological change in the Fermi surface related to the passage of an extremum of the electron energy band (equivalent to the van Hove peak in the density of states) through the Fermi level [65]. Fig. 5c indicates, at 2.3 GPa, the *Pnnm* phase shows a semimetallic band structure with the hole band along  $\Gamma$ -X symmetry line, which induces the hole transport along the *b* direction. The crossing of bands probably causes a pressure-induced ETT in *Pnnm* phase. As shown in Fig. S5b, the bands crossing states are mainly composed by Se1, In4 and In2 electrons. At 3.5 GPa, the *Pnnm* phase becomes

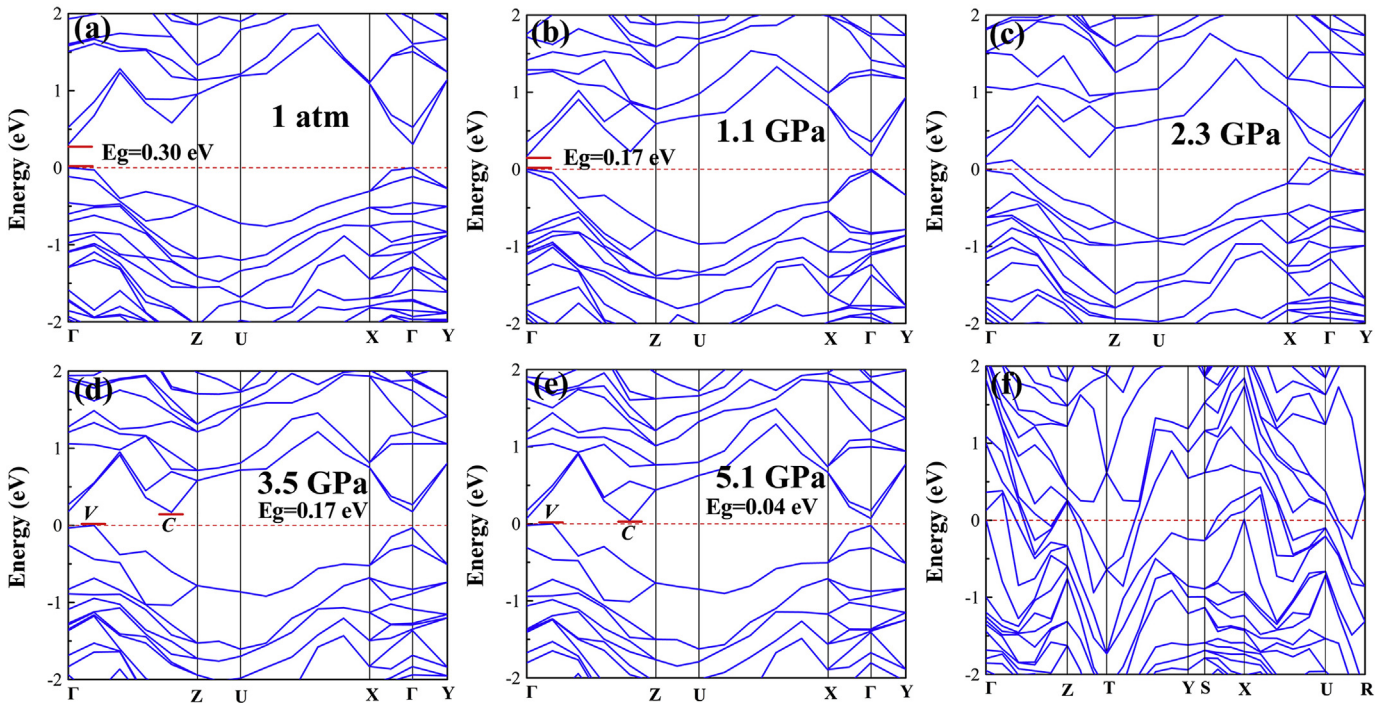


**Fig. 5.** Calculated band structures of  $\text{In}_4\text{Se}_3$  for (a) ambient pressure, (b) 1.1 GPa, (c) 2.3 GPa, (d) 3.5 GPa, (e) 5.1 GPa and (f) the  $\text{Pca}_{21}$  phase, respectively.

an indirect band-gap semiconductor with CBM at around  $Z$  point (C) and VBM at around  $\Gamma$  point (V),  $Eg = 0.17$  eV, as shown in Fig. 5d. Fig. S5c shows the VBM of 3.5 GPa is mostly due to the contributions of  $\text{In}4\text{-s}$ ,  $\text{Se}2\text{-p}$  and  $\text{Se}3\text{-p}$  states. Due to the opening-up of band-gap at 3.5 GPa, the  $\text{Pnnm}$  phase experiences a possible pressure-induced ETT once more. Because it is not obvious that quasi-one-dimensional Fermi surface nesting conditions related with CDW instability may be conserved in the whole range of stability of the low pressure phase. So, the semiconducting state which appears above 3.5 GPa may contain CDW but maybe not. As the crystal structure does not change and stay anisotropic, CDW is possible. Note that a sudden increase in CDW order was observed previously in  $\text{TaS}_2$  and  $\text{TaSe}_2$  at pressure, due to the lock-in transition from incommensurate CDW to commensurate CDW [40,66]. The possible CDW → semimetal → CDW transition was uncovered for the first time in the CDW system studies. As shown in Fig. 5e, by the raised pressure, the band-gap reduces to 0.04 eV at 5.1 GPa. The large band overlap was observed in the band structures of the  $\text{Pca}_{21}$  phase, which shows the  $\text{Pca}_{21}$  phase is a bulk metal state, see Fig. 5f.

Besides, due to the ETTs are shown to strongly influence the thermoelectrical properties in compounds, we would like to discuss about the thermoelectrical property of the  $\text{Pnnm}$  phase after ETTs [44–52]. It is worth mentioning that although there is low thermal conductivity in a CDW system, it is crucial to select one type of carrier transport (electron or hole) to achieve a high thermopower, because mixed carrier transport (electrons and holes) suppresses the Seebeck coefficient [20]. At 5.1 GPa, due to the CBM and the second CBM is very close in energy, see Fig. 5e, the phonon-assisted intervalley scattering of electron was dramatically enhanced. The anisotropic transport of carriers and electron's intervalley scattering phenomenon can prevent the electron-hole compensation effect in Seebeck coefficients [22]. Thus, a considerable increase in Seebeck coefficient was expected by the contribution of single carrier (holes) transport. Furthermore, due to the low band-gap at above 5.1 GPa, a remarkable increase of carrier concentration and electrical conductivity can be obtained.

Therefore, an improvement of the  $ZT$  value can be expected in the  $\text{Pnnm}$  phase after ETTs.

Apart from the direct observation of the changes at the Fermi surface by means of angle-resolved photoelectron spectroscopy, transport measurements have also been used as one of the most convincing ways to detect ETTs [44–52,65]. However, the present *in situ* high-pressure temperature dependence of resistance measurement technique cannot provide the extremely exact carrier activation energy of the sample not easy to be loaded full of the pressure calibrator. Therefore, it is need to develop the *in situ* high-pressure transport measurement technique for the rather sticky sample, such as  $\text{In}_4\text{Se}_3$ . Finally, the following techniques can provide useful information on the changes of the CDW state in the  $\text{Pnnm}$  phase under pressure, such as, scanning tunneling microscope (STM), X-ray resonant scattering (XRS) and X-ray photon correlation spectroscopy (XPCS) measurements. On the other hand, the superconductivity study of the  $\text{Pnnm}$  phase could be helpful for identifying the unsettled mechanism and finding new materials with higher critical temperature by using the chemical pressure.

#### 4. Conclusions

In summary, we have investigated the structural transitions of  $\text{In}_4\text{Se}_3$  up to 48.8 GPa at room temperature by ADXRD measurements.  $\text{In}_4\text{Se}_3$  undergoes twice phase transitions at about 7.0 and 34.2 GPa, respectively. The first high-pressure phase was assigned to the  $\text{Pca}_{21}$  structure. Moreover, by means of first-principle calculations, we proposed that the  $\text{Pnnm}$  phase undergoes twice possible ETTs, from CDW state to a semimetallic state at about 2.3 GPa and then back to a possible CDW state at around 3.5 GPa. A pressure-induced metallization was attributed to the first structural transition. Besides, a decrease of the electron-hole compensation effect in Seebeck coefficient was proposed in the  $\text{Pnnm}$  phase upon compression, which can lead to a considerable increase in the  $ZT$  value.

## Acknowledgments

This work was financially supported by the National Natural Science Foundation of China (Grant Nos. 41572357).

## Appendix A. Supplementary data

Supplementary data related to this article can be found at <http://dx.doi.org/10.1016/j.jallcom.2017.04.261>.

## References

- [1] Y. Feng, J. van Wezel, J. Wang, F. Flicker, D.M. Silevitch, P.B. Littlewood, T.F. Rosenbaum, *Nat. Phys.* 11 (2015) 865.
- [2] E.H. da Silva Neto, R. Comin, F. He, R. Sutarto, Y. Jiang, R.L. Greene, G.A. Sawatzky, A. Damascelli, *Science* 347 (2015) 282.
- [3] G. Campi, A. Bianconi, N. Poccia, G. Bianconi, L. Barba, G. Arrighetti, D. Innocenti, J. Karpinski, N.D. Zhigadlo, S.M. Kazakov, M. Burghammer, M.V. Zimmermann, M. Sprung, A. Ricci, *Nature* 525 (2015) 359.
- [4] J.M. Tranquada, B.J. Sternlieb, J.D. Axe, Y. Naka-mura, S. Uchida, *Nature* 375 (1995) 561.
- [5] J. Homan, E. Hudson, K. Lang, V. Madhavan, H. Eisaki, S. Uchida, J. Davis, *Science* 295 (2002) 466.
- [6] D. LeBoeuf, N. Doiron-Leyraud, J. Levallois, R. Daou, J.-B. Bonnemaison, N.E. Hussey, L. Balicas, B.J. Ramshaw, R. Liang, D.A. Bonn, W.N. Hardy, S. Adachi, C. Proust, L. Taillefer, *Nature* 450 (2007) 533.
- [7] S.E. Sebastian, N. Harrison, E. Palm, T.P. Murphy, C.H. Mielke, R. Liang, D.A. Bonn, W.N. Hardy, G.G. Lonzarich, *Nature* 454 (2008) 200.
- [8] T. Wu, H. Mayaffre, S. Krämer, M. Horvatić, C. Berthier, W.N. Hardy, R. Liang, D.A. Bonn, M.-H. Julien, *Nature* 477 (2011) 191.
- [9] G. Ghiringhelli, M. Le Tacon, M. Minola, S. Blanco-Canosa, C. Mazzoli, N.B. Brookes, G.M. De Luca, A. Frano, D.G. Hawthorn, F. He, T. Loew, M.M. Sala, D.C. Peets, M. Salluzzo, E. Schierle, R. Sutarto, G.A. Sawatzky, E. Weschke, B. Keimer, L. Braicovich, *Science* 337 (2012) 821.
- [10] J. Chang, E. Blackburn, A.T. Holmes, N.B. Christensen, J. Larsen, J. Mesot, R. Liang, D.A. Bonn, W.N. Hardy, A. Watenphul, M.V. Zimmermann, E.M. Forgan, S.M. Hayden, *Nat. Phys.* 8 (2012) 871.
- [11] E.H. da Silva Neto, P. Aynajian, A. Frano, R. Comin, E. Schierle, E. Weschke, A. Gynis, J. Wen, J. Schneeloch, Z. Xu, S. Ono, G. Gu, M. Le Tacon, A. Yazdani, *Science* 343 (2014) 393.
- [12] R. Comin, A. Frano, M.M. Yee, Y. Yoshida, H. Eisaki, E. Schierle, E. Weschke, R. Sutarto, F. He, A. Soumyanarayanan, Y. He, M. Le Tacon, I.S. Elmov, J.E. Homan, G.A. Sawatzky, B. Keimer, A. Damascelli, *Science* 343 (2014) 390.
- [13] K. Fujita, M.H. Hamidian, S.D. Edkins, C.K. Kim, Y. Kohsaka, M. Azuma, M. Takano, H. Takagi, H. Eisaki, S.-i. Uchida, A. Allais, M.J. Lawler, E.A. Kim, S. Sachdev, J.C.S. Davis, *Proc. Natl. Acad. Sci. U. S. A.* 111 (2014) E3026.
- [14] V. Thampy, M.P.M. Dean, N.B. Christensen, L. Steinke, Z. Islam, M. Oda, M. Ido, N. Momono, S.B. Wilkins, J.P. Hill, *Phys. Rev. B* 90 (2014) 100510.
- [15] N.B. Christensen, J. Chang, J. Larsen, M. Fujita, M. Oda, M. Ido, N. Momono, E. M. Forgan, A. T. Holmes, J. Mesot, M. Huecker, M. v. Zimmermann, arXiv: 1404.3192 (unpublished).
- [16] T.P. Croft, C. Lester, M.S. Senn, A. Bombardi, S.M. Hayden, *Phys. Rev. B* 89 (2014) 224513.
- [17] W. Tabis, Y. Li, M. Le Tacon, L. Braicovich, A. Kreysig, M. Minola, G. Dellea, E. Weschke, M.J. Veit, M. Ramazanoglu, A.I. Goldman, T. Schmitt, G. Ghiringhelli, N. Barisić, M.K. Chan, C.J. Dorow, G. Yu, X. Zhao, B. Keimer, M. Greven, *Nat. Commun.* 5 (2014) 5875.
- [18] R. Comin, A. Damascelli, *Annu. Rev. Condens. Matter Phys.* 7 (2016) 369.
- [19] M. Eichberger, H. Schäfer, M. Krumova, M. Beyer, J. Demsar, H. Berger, G. Moriena, G. Sciaiini, R.J.D. Miller, *Nature* 468 (2010) 799.
- [20] J.-S. Rhyee, K.H. Lee, S.M. Lee, E. Cho, S.I. Kim, E. Lee, Y.S. Kwon, J.H. Shim, G. Kotliar, *Nature* 459 (2009) 965.
- [21] H.S. Ji, H. Kim, C. Lee, J.-S. Rhyee, M.H. Kim, M. Kaviani, J.H. Shim, *Phys. Rev. B* 87 (2013) 125111.
- [22] J. Rhyee, E. Cho, K.H. Lee, S.M. Lee, S.I. Kim, H. Kim, Y.S. Kwon, S.J. Kim, *Appl. Phys. Lett.* 95 (2009) 212106.
- [23] D.M. Bercha, K.Z. Rushchanskii, M. Sznajder, *Phys. Status Solidi B* 212 (1999) 247.
- [24] N. Benramdane, A. Bouzidi, H. Tabetderraz, Z. Kebab, M. Latreche, *Micro Eng.* 51–52 (2000) 645.
- [25] T. Gertovich, S. Grineva, B. Gritsiuk, A. Ogorodnika, O. Stoliarchuk, K. Tovstiuk, *Ukr. Fiz. Zh. Russ. Ed.* 27 (1982) 1191.
- [26] P. Galij, T. Nenchuk, O. Dveriy, A. Ciszewski, P. Mazur, S. Zuber, *Phys. E* 41 (2009) 465.
- [27] N. Benramdane, R. Musho, *Sol. Energy Mater. Sol. Cells* 37 (1995) 367.
- [28] T. Melnychuk, V. Strebegov, G. Vorobets, *Appl. Surf. Sci.* 254 (2007) 1002.
- [29] L. Makinistian, E.A. Albanesi, N.V. Gonzalez Lemus, A.G. Petukhov, D. Schmidt, E. Schubert, M. Schubert, Ya. B. Losovyj, P. Galij, P. Dowben, *Phys. Rev. B* 81 (2010) 075217.
- [30] X.J. Chen, V.V. Struzhkin, Y. Yu, A.F. Goncharov, C.T. Lin, H.K. Mao, R.J. Hemley, *Nature* 466 (2010) 950.
- [31] S. Sadewasser, J.S. Schilling, A.P. Paulikas, B.W. Veal, *Phys. Rev. B* 61 (2000) 741.
- [32] X.-J. Chen, V.V. Struzhkin, R.J. Hemley, H.K. Mao, C. Kendziora, *Phys. Rev. B* 70 (2004) 214502.
- [33] R. Kubiak, K. Westerholz, H. Bach, *Phys. C* 166 (1990) 523.
- [34] L. Gao, Y.Y. Xue, F. Chen, Q. Xiong, R.L. Meng, D. Ramirez, C.W. Chu, J.H. Eggert, H.K. Mao, *Phys. Rev. B* 50 (1994) 4260.
- [35] A. Sacchetti, E. Arcangeletti, A. Perucchi, L. Baldassarre, P. Postorino, S. Lupi, N. Ru, I.R. Fisher, L. Degiorgi, *Phys. Rev. Lett.* 98 (2007) 026401.
- [36] O. Cyr-Choinière, D. LeBoeuf, S. Badoux, S. Dufour-Beausejour, D. A. Bonn, W. N. Hardy, R. Liang, N. Doiron-Leyraud, L. Taillefer, arXiv: 1503.02033 (unpublished).
- [37] M. Houcker, M. v. Zimmermann, M. Debessai, J.S. Schilling, J.M. Tranquada, G.D. Gu, *Phys. Rev. Lett.* 104 (2010) 057004.
- [38] M. Abdel-Hafiez, X.-M. Zhao, A.A. Kordyuk, Y.-W. Fang, B. Pan, Z. He, C.-G. Duan, J. Zhao, X.-J. Chen, *Sci. Rep.* 6 (2016) 31824.
- [39] H. Suderow, V.G. Tissen, J.P. Brison, J.L. Martínez, S. Vieira, *Phys. Rev. Lett.* 95 (2005) 117006.
- [40] D.C. Freitas, P. Rodière, M.R. Osorio, E. Navarro-Moratala, N.M. Nemes, V.G. Tissen, L. Cario, E. Coronado, M. García-Hernández, S. Vieira, M. Núñez-Regueiro, H. Suderow, *Phys. Rev. B* 93 (2016) 184512.
- [41] C. Berthier, P. Molinié, D. Jérôme, *Solid State Commun.* 18 (1976) 1393.
- [42] Y.I. Joe, X.M. Chen, P. Ghaemi, K.D. Finkelstein, G.A. de la Pea, Y. Gan, J.C.T. Lee, S. Yuan, J. Geck, G.J. MacDougall, T.C. Chiang, S.L. Cooper, E. Fradkin, P. Abbamonte, *Nat. Phys.* 10 (2014) 421.
- [43] X.M. Chen, V. Thampy, C. Mazzoli, A.M. Barbour, H. Miao, G.D. Gu, Y. Cao, J.M. Tranquada, M.P.M. Dean, S.B. Wilkins, *Phys. Rev. Lett.* 117 (2016) 167001.
- [44] Y.H. Zhang, Y. Li, Y.M. Ma, Y.W. Li, G.H. Li, X.C. Shao, H. Wang, T. Cui, X. Wang, P.W. Zhu, *Sci. Rep.* 5 (2015) 14681.
- [45] M. Jacobsen, S. Sinogeikin, R. Kumar, A. Cornelius, *J. Phys. Chem. Solids* 73 (2012) 1154.
- [46] Y.H. Zhang, Y.M. Ma, A.H. Geng, C.Y. Zhu, G.T. Liu, Q. Tao, F. Li, Q.L. Wang, Y. Li, X. Wang, P.W. Zhu, *J. Alloys Compd.* 685 (2016) 551.
- [47] S.V. Ovsyannikov, V.V. Shchennikov, *Chem. Mater.* 22 (2010) 635.
- [48] F.J. Manjón, R. Vilaplana, O. Gomis, E. Pérez-González, D. Santamaría-Pérez, V. Marin-Borrás, A. Segura, J. González, P. Rodríguez-Hernández, A. Muñoz, C. Drasar, V. Kucek, V. Muñoz-Sanjosé, *Phys. Status Solidi B* 250 (2013) 669.
- [49] E. Itskevich, L. Kashirskaya, V. Kraidenov, *Semiconductors* 31 (1997) 276.
- [50] C.N. Shekar, D. Polvani, J. Meng, J. Badding, *Phys. B* 358 (2005) 14.
- [51] N. Sakai, H. Fritzsche, *Phys. Rev. B* 15 (1977) 973.
- [52] T.J. Scheideman, J.F. Meng, J.V. Badding, *J. Phys. Chem. Solids* 66 (2005) 1744.
- [53] U. Schwarz, H. Hillebrecht, H.J. Deiseroth, R. Walther, Z. Krist. 210 (1995) 342.
- [54] G. Li, J. Yang, Y. Luo, Y. Xiao, L. Fu, M. Liu, J. Peng, *J. Am. Ceram. Soc.* 96 (2013) 2703.
- [55] H. Mao, J.-A. Xu, P. Bell, *J. Geophys. Res.* 91 (1986) 4673.
- [56] A.P. Hammersley, S.O. Svensson, M. Hanfland, A.N. Fitch, D. Hausermann, *High. Press. Res.* 14 (1996) 235.
- [57] A.C. Larson, R.B. Von Dreele, *General Structure Analysis System, LANSCE*, MS-H805, Los Alamos, New Mexico, 1994.
- [58] B.H. Toby, *J. Appl. Crystallogr.* 34 (2001) 210.
- [59] Y. Wang, J. Lv, L. Zhu, Y. Ma, *Phys. Rev. B* 82 (2010) 094116.
- [60] G. Kresse, J. Furthmüller, *Phys. Rev. B* 54 (1996) 11169.
- [61] J.P. Perdew, K. Burke, M. Ernzerhof, *Phys. Rev. Lett.* 77 (1996) 3865.
- [62] G. Kresse, D. Joubert, *Phys. Rev. B* 59 (1999) 1758.
- [63] P.E. Blöchl, *Phys. Rev. B* 50 (1994) 17953.
- [64] F. Birch, *J. Appl. Phys.* 9 (1938) 279.
- [65] R. Vilaplana, J.A. Sans, F.J. Manjón, A. Andrade-Chacon, J. Sanchez-Benítez, O. Gomis, A.I.J. Pereira, B. García-Domene, P. Rodríguez-Hernandez, A. Munoz, D. Daisenberger, O. Oeckler, *J. Alloys Compd.* 685 (2016) 962.
- [66] D.B. McWhan, R.M. Fleming, D.E. Moncton, F.J. DiSalvo, *Phys. Rev. Lett.* 45 (1980) 269.